Eur. Phys. J. C 12, 507–520 (2000)
Digital Object Identifier (DOI) 10.1007/s100529900262

THE EUROPEAN PHYSICAL JOURNAL C

Neutrino masses, mixing angles and the unification of couplings in the MSSM

M. Carena[1,a], J. Ellis[1], S. Lola[1], C.E.M. Wagner[1,2]

[1] Theory Division, CERN, 1211 Geneva, Switzerland
[2] Argonne National Laboratory, 9700 Cass Ave., Argonne, IL 60439, USA

Received: 22 June 1999 / Published online: 10 December 1999

Abstract. In the light of the gathering evidence for $\nu_\mu - \nu_\tau$ neutrino oscillations, coming in particular from the Super-Kamiokande data on atmospheric neutrinos, we re-analyze the unification of gauge and Yukawa couplings within the minimal supersymmetric extension of the Standard Model (MSSM). Guided by a range of different grand-unified models, we stress the relevance of large mixing in the lepton sector for the question of bottom-tau Yukawa coupling unification. We also discuss the dependence of the favoured value of $\tan\beta$ on the characteristics of the high-energy quark and lepton mass matrices. In particular, we find that, in the presence of large lepton mixing, Yukawa unification can be achieved for intermediate values of $\tan\beta$ that were previously disfavoured. The renormalization-group sensitivity to the structures of different mass matrices may enable Yukawa unification to serve as a useful probe of GUT models.

1 Introduction

The most mysterious aspect of the Standard Model may be the pattern of fermion masses and mixing. These are characterized by many parameters, whose patterns are difficult to discern. Two major classes of theoretical approaches to the question of fermion masses may be distinguished: Grand Unified Theories (GUTs), whose non-Abelian gauge symmetries may relate the masses of fermions in the same generation via Clebsch-Gordan coefficients of order unity, that are renormalized in a calculable way, and global flavour symmetries such as U(1), which may explain the observed hierarchies of fermion masses and mixing between different generations. The first (and only successful) GUT mass prediction was that $m_b = m_\tau$ before renormalization [1], which is compatible with the measured values at the $\sim$ 10–30% level, in both the Standard Model and the Minimal Supersymmetric Standard Model (MSSM) [2]. Optimal agreement within the MSSM is found either for $\tan\beta \leq 2$ or for $\tan\beta \geq 30$, with the attractive possibility of $b-\tau-t$ Yukawa coupling unification in the latter case [3–5]. The naïve parallel predictions $m_s = m_\mu$ and $m_d = m_e$ are unsuccessful, but these may be modified by non-trivial Clebsch-Gordan coefficients [6] and/or higher-dimensional contributions [7] to the fermion mass matrices controlled by global U(1) flavour symmetries.

Important new information is now being provided by the emerging pattern of neutrino masses and mixing [8,9]. Various predictions for these had been made in the context of different models for quark and lepton masses [10, 11], which are now being winnowed out by the experimental measurements. In particular, the possibility that the Maki-Nakagawa-Sakata (MNS) [12] lepton mixing angles might be large had not always been anticipated, and raise questions about the viability of the successful prediction $m_b = m_\tau$. The purpose of this paper is to explore the circumstances under which this prediction can be retained, based on a study of generic patterns of mixing among neutrino and charged-lepton flavours, and to understand the corresponding flexibility in the range of $\tan\beta$ compatible with $b-\tau$ Yukawa unification and other hypotheses.

Our work has been stimulated by reports from the Super-Kamiokande Collaboration [8], which are also supported by other experiments [9], that confirm previous measurements that the ν_μ/ν_e ratio in atmospheric neutrinos is smaller than the Standard Model expectations. The existing data favour [8,13] ν_μ–ν_τ oscillations, with the following constraints on the mass differences and the mixing:

$$\delta m^2_{\nu_\mu\nu_\tau} \approx (10^{-2} \text{ to } 10^{-3}) \text{ eV}^2 \quad (1)$$

$$\sin^2 2\theta_{\mu\tau} \geq 0.9 \,. \quad (2)$$

If one departs from the Standard Model and assumes the existence of non-zero neutrino masses, it is natural also to resolve the solar-neutrino deficit through neutrino oscillations. In the case of vacuum oscillations, one requires large mixing and a splitting between the oscillating neutrinos in the range $\delta m^2_{\nu_e\nu_\alpha} \approx (0.5-1.1)\times 10^{-10}$ eV^2, where α is μ or τ. On the other hand, matter-enhanced oscillations

[a] On leave of absence from Fermi National Accelerator Laboratory, Batavia, IL 60510, USA

[14] within the Sun would allow for both small and large mixing, with $\delta m^2_{\nu_e \nu_\alpha} \approx (0.3 - 20) \times 10^{-5}$ eV^2 [1].

The most straightforward extension of the Standard Model that one may consider is to include three new right-handed neutrino states, with Yukawa couplings similar to those of the other fermions. The easiest way to explain the smallness of the neutrino masses is then to assume that the right-handed neutrinos acquire a gauge-invariant but lepton-number-violating Majorana mass of the type $M_{\nu_R} \nu_R \nu_R$, with $M_{\nu_R} \gg M_W$. Neutrino masses are then determined via a see-saw mechanism [17], with the light neutrino eigenvalues being determined by the diagonalization of the matrix

$$M = \begin{pmatrix} 0 & m_\nu^D \\ m_\nu^{D^T} & M_{\nu_R} \end{pmatrix} \tag{3}$$

to be $m_{light} \simeq \frac{(m_\nu^D)^2}{M_{\nu_R}}$, where m_ν^D is the Dirac neutrino mass matrix, and hence naturally suppressed.

Since both the solar and atmospheric deficits require small mass differences, there are two possible neutrino hierarchies that could explain them simultaneously:

a) Textures with almost degenerate neutrino eigenstates, with mass $\mathcal{O}$(eV). In this case neutrinos may also provide astrophysical hot dark matter, and

b) Textures with large hierarchies of neutrino masses: $m_3 \gg m_2 \gg m_1$, in which case the atmospheric neutrino data require $m_3 \approx$ (0.03 to 0.1) eV and $m_2 \approx (10^{-2}$ to $10^{-3})$ eV.

In this article, we shall concentrate on this second possibility, motivated in part by the difficulties thrown up by renormalization effects in models with degenerate neutrinos [18,19].

As we have emphasized, one of the major challenges in high-energy physics is the origin of the fermion masses and mixing angles, and the neutrino data are now providing us with precious new information. It is interesting to investigate if the pattern of neutrino masses and mixing angles may be accomodated in a natural way within a GUT scenario [20–23], with supersymmetry realized at low energies. Indeed, the successful unification of gauge couplings provides one of the main experimental motivations for low-energy supersymmetry. For values of $\alpha_3(M_Z) \simeq 0.118$, gauge-coupling unification is accurate for a supersymmetric spectrum with masses of the order of 1 TeV, whereas, as we said above, in the absence of neutrino masses, $b - \tau$ mass unification demands either small values of $\tan\beta$, close to the infrared fixed-point solution of the MSSM renormalization-group equations, or large values of $\tan\beta$ [24,4,25,26].

In the presence of neutrino masses, the running of the various couplings from the unification scale down to low energies is modified. From M_{GUT} to the scale M_N, at which the effective light-neutrino mass operator appears, the effects of the neutrino Yukawa coupling essentially cancel those of the top Yukawa coupling in the m_b/m_τ ratio, if one assumes unification of the third-generation neutrino and top Yukawa couplings. This makes precise unification hard to achieve [27,28]. However, it was shown in [29] that precise unification can be restored in the presence of large lepton mixing. Since the right handed neutrinos are neutral, the unfication of gauge couplings is only affected by the presence of the Dirac Yukawa coupling at the two-loop level. The largest effects are obtained for values of the neutrino masses such that the neutrino Yukawa coupling becomes strong, close to the limit of perturbativity, at scales of the order of M_{GUT}. The effect of the neutrino Yukawa coupling lowers the predicted value of strong gauge coupling, $\alpha_3(M_Z)$, by less than one percent. Below, we make an extensive study of the unification of couplings, taking into account the information available from Super-Kamiokande and other neutrino experiments.

Below M_N, the ν_R decouple from the spectrum, and the quantity that gets renormalized is an effective neutrino operator of the type $\nu_L \nu_L H H$ [30,31]. Renormalization-group effects, which may be summarized by simple semi-analytic expressions both in the ranges M_{GUT} to M_N [29] and M_N to low energies [32,33,18], may give important information on the structure of the neutrino textures. Different boundary conditions for the Yukawa couplings of the third generation of quarks and leptons at M_{GUT} and the precise value of M_N may constrain, for different ranges of $\tan\beta$ [29,18,19], the amount of mixing in the lepton sector. Quite generically, a given amount of mixing at the GUT scale may be amplified or destroyed at low energies, and vice versa, due to strong renormalization-group effects.

In the present work, we analyze in a systematic way the implications of the recent experimental information on neutrino masses and mixing for the unification of couplings at a high energy scale. We shall concentrate on the small and moderate $\tan\beta$ regime, in which the impact of the lepton mixing on the question of unification of coupling becomes most relevant. We review in Sect. 2 our theoretical framework for analyzing fermion textures, which is a generic supersymmetric $SO(10)$ GUT with higher-dimensional interactions. We use this to establish examples of different possible origins of large neutrino mixing. In Sect. 3, we analyze the renormalization-group running of quark, lepton and neutrino masses below the GUT scale M_{GUT}, both above and below the intermediate seesaw mass scale M_N, establishing the conditions for maximal neutrino mixing. In Sect. 4, we present numerical results which show how the successful prediction $m_b = m_\tau$ may be retained, even for intermediate values of $\tan\beta$ that were previously disfavoured in the MSSM. In Sect. 5 we analyse the results of using the precise $SU(5)$ relations between the mixing of the left-handed leptons and the right-handed down-quark states. Finally, in Sect. 6 we summarize our conclusions and identify outstanding issues for future study.

[1] We do not pursue here evidence from the LSND Collaboration for $\bar{\nu}_\mu$–$\bar{\nu}_e$ and ν_μ–ν_e oscillations [15], which has not yet been confirmed by the KARMEN 2 experiment [16].

2 Theoretical framework for fermion textures

We now discuss examples how the classes of mass matrices that we study, embodying bottom-tau unification at the GUT scale, may be realized. As already stressed, the hierarchical structure of the fermion mass matrices suggests that they might be generated by an underlying family symmetry. The various Standard Model fields would have certain charges under this symmetry, and a coupling represented by a given operator is allowed if its net flavour charge is zero. Since the top, bottom and τ masses are larger than the rest of the fermion masses with the same quantum numbers, a natural expectation is that they arise via renormalizable terms. The remaining entries are hypothesized to be generated from higher-dimensional operators when the flavour symmetry is spontaneously broken, via vev's for fields that are singlets of the Standard Model gauge group, with non-trivial flavour charge. Precise unification of the bottom and tau masses may take place if we work within a GUT scheme, which may lead to specific Clebsch-Gordan relations between the couplings of quarks and leptons. Since, it is important for our purposes to know the exact relation between $\lambda_b(M_{GUT})$ and $\lambda_\tau(M_{GUT})$, we now describe a framework where exact $b-\tau$ unification is guaranteed, whilst the mixing in the left-handed lepton sector may be quite different from that in the right-handed down-quark sector.

As a specific example of a GUT symmetry that unifies quarks and leptons in common representations, leading to various relations between the charges of the quark and lepton fields, and hence to relations between their mass hierarchies, we consider $SO(10)$ models, for which it has already been shown that maximal ν_μ-ν_τ mixing can be generated [34] [2]. A feature of this model approach is that one can also account for the mass splitting within a particular family. Realistic mass matrices may be obtained by considering the effects of the Higgs multiplets that are necessary in order to break $SO(10)$ to $SU(3)\times SU(2)\times U(1)$ [35]. The smallest such representations are **45**, **16** and $\overline{\mathbf{16}}$, which may be used to generate operators with rank ≥ 4 in the mass matrices. Along these lines, one can use the $SO(10)$-invariant Yukawa interaction $O_{33} = A\cdot\mathbf{16}_3\,\mathbf{10}\,\mathbf{16}_3$ to give mass to the fermions of the third family in terms of a single coupling A. Higher-order operators are of the general type

$$O_{ij} = \mathbf{16}_i \ \frac{M_{GUT}^k \ \mathbf{45}_{k+1}\cdots\mathbf{45}_m}{M_P^l \ \mathbf{45}_X^{m-l}} \cdot\mathbf{10} \ \frac{M_G^n \ \mathbf{45}_{n+1}\cdots\mathbf{45}_p}{M_P^q \ \mathbf{45}_X^{p-q}} \ \mathbf{16}_j \qquad (4)$$

where the **45** representations in the numerator are along any of the four directions $X, Y, B-L, T_{3R}$ [3]. The mass terms of the first and second fermion families are generated from particular non-renormalizable operators, whose coefficients are suppressed by a set of large scales. Whether the mass matrices will be symmetric or non-symmetric depends on the choice of operators. We concentrate in this paper on models with symmetric mass matrices, since these are sufficient to illustrate our key points: our analysis could easily be extended to include non-symmetric cases.

Table 1. $X, Y, B-L$ and T_{3R} quantum numbers of the Standard Model fermions

	X	Y	$B-L$	T_{3R}
q	1	1	1	0
u^c	1	-4	-1	1
d^c	-3	2	-1	-1
ℓ	-3	-3	-3	0
e^c	1	6	3	-1
ν^c	5	0	3	1

Each direction in $SO(10)$ is associated with different quantum numbers for different family members, which can give different but related coefficients between the quark and lepton mass matrices. For completeness, we present these coefficients in Table 1. As we see from the Table 1, the absolute values of the coefficients of interest vary from 0 to 6, indicating that we can in principle obtain very different hierarchies between the textures of quark and lepton masses. Taking into account the known low-energy data, acceptable models have been identified [35,36], within which the lower 2×2 up-, down-quark and charged-lepton mass matrices are written as

$$m_{U,D,E} \propto \begin{pmatrix} y_a E e^{i\phi} & x_a^{'} B \\ x_a B & A \end{pmatrix}, \qquad (5)$$

where x_a, $x_a^{'}$ and y_a are Clebsch-Gordan factors, whilst A, B, E and ϕ are arbitrary parameters, with $A \gg B, E$ being adjusted by the fermion data. These textures can be generated both in the large [35] and small [36] $\tan\beta$ regimes (for the latter case, see Appendix A).

Following the Super-Kamiokande data, we require in addition large mixing in the (23) lepton sector, while the (23) quark mixing is small. Moreover, we need $\frac{m_\mu}{m_\tau} > \frac{m_s}{m_b}$, as well as certain cancellations between the various entries in the lepton sector, in order to obtain the correct $\frac{m_\mu}{m_\tau}$ ratio. There is some freedom to achieve the desired cancellations by an appropriate choice of E and y_a, however the chosen operators have also to match the quark data. In what follows, we will try to identify some viable examples, without doing a complete operator analysis.

[2] Analogous studies could be made in the context of flipped $SU(5)\times U(1)$: see [32] and references therein.

[3] In particular, the **45** is the adjoint representation of $SO(10)$, and therefore its vev may point in any direction in the space of the 45 generators of $SO(10)$, as long as it leaves the standard model gauge group unbroken. A vev in the X direction is required for the breakdown of $SO(10)$ to $SU(5)\times U(1)_X$ at a scale M_{10} between M_{GUT} and M_P. The other directions are associated with the breaking of $SU(5)$ down to the Standard Model gauge group.

There are in principle two ways to obtain the correct lepton and quark contributions simultaneously:

(i) The easiest way to search for suitable operators is to assume that the operators contributing to the (23) and (32) elements are such that the Clebsch-Gordan factors controlling the lepton mass matrix elements are much larger than the quark ones. These operators are then assumed to lead to the relevant lepton entries, whilst the associated up- and down-quark terms could come either from these same operators or from other subleading ones.

(ii) One can add two different operators, in a way that cancellations are achieved. The difficulty in this case is that the vev's and coefficients of two different operators need to match quite well in order to lead to the desired results.

We first concentrate on the measured (23) lepton mixing. This can arise either from the charged-lepton sector, or the neutrino sector, or both. Indeed, the leptonic mixing matrix V_{MNS} of Maki, Nakagawa and Sakata [12] is defined in a way similar to the Cabibbo-Kobayashi-Maskawa mixing matrix V_{CKM} for the quark currents:

$$V_{MNS} = V_\ell V_\nu^\dagger \tag{6}$$

where V_ℓ transforms the left-handed charged leptons to a diagonal mass basis, whereas V_ν diagonalizes the light-neutrino mass matrix [17],

$$m_{eff} = m_\nu^D \cdot (M_{\nu_R})^{-1} \cdot m_\nu^{D^T}. \tag{7}$$

In the above m_ν^D is the Dirac neutrino mass matrix and M_{ν_R} the heavy Majorana mass matrix. We assume that the lepton mass hierarchy originates from the structure of the Dirac neutrino and charged-lepton mass matrices. Quite generally, under these conditions, the structure of the heavy Majorana mass matrix M_{ν_R} does not affect the low-energy lepton mixing (see Appendix B). We further concentrate on the case (i) discussed above, looking for operators of relatively low order, so that they are not suppressed by the high scales of the theory. For simplicity of presentation, we impose the requirement of symmetric mass matrices, which constrains the possible choices.

We remark that the lower-order symmetric operators with Clebsch-Gordan factors with large differences between quarks and leptons tend to lead to similar mixing angles in the charged-lepton and neutrino sectors, and hence to small lepton mixing. This is, e.g., the case with the operator

$$\mathbf{16}\ \mathbf{45}_{B-L}\ \mathbf{10}\ \mathbf{45}_{B-L}\ \mathbf{16}, \tag{8}$$

which leads to Clebsch-Gordan factors $x_u = x_d = -1$ and $x_\ell = x_\nu = -9$. On the other hand, there also exist operators that lead to large differences between the individual quark and lepton Clebsch-Gordan coefficients, and, due to cancellations in the quark sector, lead to a small mixing angle between the second- and third-generation quarks. Some examples of these operators that can lead to the desired hierarchies between the lepton and quark matrix elements are shown in Table 2.

Moreover, we also observe the following:

• There exist higher-order operators that can be less suppressed than others, under certain conditions. For example, consider terms of the form

$$\mathbf{16}\ \mathbf{45}_i\ \mathbf{10}\ \frac{\mathbf{45}_j}{\mathbf{45}_X}\ \frac{\mathbf{45}_k}{\mathbf{45}_X}\ \mathbf{10} + \text{symmetrizing term},$$

where i, j, k can be any of the $Y, B-L$ and T_{3R} directions. If the vev's along the $Y, B-L$, T_{3R} and X directions are not very different, these terms can be relatively unsuppressed. We tabulate some such operators that lead to significantly lepton mixing significanmtly larger than the quark mixing in Table 3. We observe that, in these cases, the lepton mixing tends to be dominated by the charged-lepton contribution. This is due to the large X Clebsch-Gordan coefficient of the right-handed neutrinos, as compared to the charged leptons, which suppresses the contributions once we start dividing by powers of $\mathbf{45}_X$. The same suppression occurs for the down-quark contributions, for this particular type of term.

Finally, one may consider operators that are suppressed by powers of the unknown fundamental scale, which may be of order of M_{GUT} models inspired by M-theory. Some examples of these are shown in Table 4.

What about the (22) elements in the mass matrices? Once we fix the (23) entries so as to obtain large lepton mixing, the (22) ones need to fall into the following pattern. For the up-quark mass matrix, we need the ratio of the (22) and (33) elements to be smaller than 1/100 (we can expect to obtain the charm mass from the off-diagonal elements in the (23) sector) [35]. In the down-quark mass matrix, the (23) element contribution to the strange mass has to be suppressed in order to be consistent with the magnitude of $V_{CKM}^{23,32}$ (in the absence of cancellations), so m_s most probably arises from the (22) element, implying again a very small ratio $m_D(22)/m_D(33)(M_{GUT})$. Finally, we require certain cancellations between the various entries in the lepton sector, in order to obtain the correct m_μ/m_τ ratio, and this leads to values of $m_E(22)/m_E(33)(M_{GUT})$ which are typically much larger than the corresponding ratios in the quark sector. To obtain these relations, we can

(a) use operators with similar structures to those displayed in Tables 3 and 4, considering also the possibility of adding extra powers of the corresponding adjoint Higgs insertions in order to get the correct relations between the (22) and (23) elements, or

(b) go to higher-order operators, with different structures from that presented above. However, a detailed operator analysis along these lines is beyond the scope of this paper.

Finally, we stress again that, in any multi-scale model like the one discussed above, the particular operators that appear will be determined by the underlying symmetry. For instance, one can combine a gauged $U(1)$ family symmetry with unification in the form of an extended vertical gauge symmetry [37]. In this case, the mass hierarchies in a fermion mass matrix are determined by the family symmetry, whilst the splittings between different

Table 2. Low-order operators that, due to cancellations in the quark sector, lead to acceptable range of values for the $V^{23}_{CKM}/V^{23}_{MNS}$ ratio, where V_{MNS} is defined in (6), despite having smaller differences between the individual quark and lepton Clebsch-Gordan coefficients

Low-Order Operators	Clebsch-Gordan Factors
$\mathbf{16}\ \mathbf{45}_X\ \mathbf{10}\ \frac{\mathbf{45}_Y}{\mathbf{45}_X}\ \mathbf{16}\ +\ \mathbf{16}\ \frac{\mathbf{45}_Y}{\mathbf{45}_X}\ \mathbf{10}\ \mathbf{45}_X\ \mathbf{16}$	$x_u=-3,\ x_d=-\frac{11}{3},\ x_\ell=-17,\ x_\nu=\ 5$
$\mathbf{16}\ \frac{\mathbf{45}_{B-L}}{\mathbf{45}_X}\ \frac{\mathbf{45}_{B-L}}{\mathbf{45}_X}\ \mathbf{10}\ \mathbf{16}\ +\ \mathbf{16}\ \mathbf{10}\ \frac{\mathbf{45}_{B-L}}{\mathbf{45}_X}\ \frac{\mathbf{45}_{B-L}}{\mathbf{45}_X}\ \mathbf{16}$	$x_u=\ 2,\ x_d=\ \frac{10}{9},\ x_\ell=10,\ x_\nu=\ \frac{34}{25}$

Table 3. Illustrative symmetric higher-order operators leading to lepton mass-matrix entries that are much larger than the corresponding quark ones

Symmetric Higher-Order Operators	Clebsch-Gordan Factors
$\mathbf{16}\ \mathbf{45}_Y\ \mathbf{10}\ \frac{\mathbf{45}_Y}{\mathbf{45}_X}\ \frac{\mathbf{45}_{B-L}}{\mathbf{45}_X}\ \mathbf{16}\ +$ sym.con.	$x_u=0,\ x_d=\frac{16}{9},\ x_\ell=-48,\ x_\nu=0$
$\mathbf{16}\ \mathbf{45}_{B-L}\ 10\ \frac{\mathbf{45}_Y}{\mathbf{45}_X}\ \frac{\mathbf{45}_{B-L}}{\mathbf{45}_X}\ \mathbf{16}\ +$ sym.con.	$x_u=3,\ x_d=-\frac{11}{9},\ x_\ell=-51,\ x_\nu=3$
$\mathbf{16}\ \mathbf{45}_{B-L}\ \mathbf{10}\ \frac{\mathbf{45}_{B-L}}{\mathbf{45}_X}\ \frac{\mathbf{45}_{B-L}}{\mathbf{45}_X}\ \mathbf{16}\ +$ sym.con.	$x_u=0,\ x_d=-\frac{8}{9},\ x_\ell=-24,\ x_\nu=-\frac{48}{25}$

Table 4. Some illustrative operators that could be relatively unsuppressed in M-thory inspired models, which lead to domination by neutrino mixing

Higher-Dimensional Operators	Clebsch-Gordan Factors
$\mathbf{16}\ \mathbf{45}_Y\ \mathbf{10}\ \mathbf{45}_X\mathbf{45}_X\ \mathbf{16}\ +$ sym.con	$x_u=-3,\ x_d=11,\ x_\ell=51,\ x_\nu=-75$
$\mathbf{16}\ \mathbf{45}_{B-L}\ \mathbf{10}\ \mathbf{45}_X\mathbf{45}_X\ \mathbf{16}\ +$ sym.con	$x_u=0,\ x_d=8,\ x_\ell=24,\ x_\nu=-48$

charge sectors of the same family are again controlled by the Clebsch-Gordan factors. In this case as well, one predicts *exact* Yukawa unification for the third family, together with Clebsch-Gordan relations that may reproduce the fermion data.

3 Neutrino mixing and renormalization-group effects

Neutrino mixing arises in analogy to quark mixing, via a mismatch between the mass eigenstates of neutrinos and charged leptons, as seen in (6). In this section, we try to understand in more detail the possible structures of lepton mass matrices that may account for the various neutrino deficits [23,29,32,38,39]. We concentrate here on the simplest case, where the problem is well approximated by a two fermion generation analysis. To see what structures may appear at low energies, we have to run the various couplings down to low energies, taking neutrino threshold effects properly into account, as discussed in the next two subsections.

3.1 Neutrino renormalization between M_{GUT} and M_N

To study the question of unification, we shall use in the numerical analysis the full two-loop renormalization group evolution of gauge and Yukawa couplings. However, in order to understand renormalization effects between M_{GUT} and M_N, in the small-tan β regime of a supersymmetric theory where only the top and the Dirac neutrino Yukawa couplings contribute in a relevant way, it is sufficient as a first illustrative approximation to study the renormalization-group equations for the Yukawa couplings at the one-loop level [4]. These take the following form in a diagonal basis [27]:

$$\begin{aligned}
16\pi^2\frac{d}{dt}\lambda_t &= \left(6\lambda_t^2+\lambda_N^2-G_U\right)\lambda_t\\
16\pi^2\frac{d}{dt}\lambda_N &= \left(4\lambda_N^2+3\lambda_t^2-G_N\right)\lambda_N\\
16\pi^2\frac{d}{dt}\lambda_b &= \left(\lambda_t^2-G_D\right)\lambda_b\\
16\pi^2\frac{d}{dt}\lambda_\tau &= \left(\lambda_N^2-G_E\right)\lambda_\tau
\end{aligned} \tag{9}$$

[4] For another recent study of the renormalization-group equations for neutrinos, see [33].

where $\lambda_\alpha : \alpha = t, b, \tau, N$, represent the third-generation Dirac Yukawa couplings for the up and down quarks, charged lepton and neutrinos, respectively, and the $G_\alpha \equiv \sum_{i=1}^{3} c_\alpha^i g_i(t)^2$ are functions that depend on the gauge couplings, with the coefficients c_α^i given in [27]. In terms of the various Yukawa couplings λ_{t_0}, λ_{N_0},λ_{b_0}, λ_{τ_0}, at the unification scale, we have

$$\lambda_t(t) = \gamma_U(t)\lambda_{t_0}\xi_t^6\xi_N \qquad \lambda_N(t) = \gamma_N(t)\lambda_{t_0}\xi_t^3\xi_N^4 \tag{10}$$

$$\lambda_b(t) = \gamma_D(t)\lambda_{b_0}\xi_t \qquad \lambda_\tau(t) = \gamma_E(t)\lambda_{\tau_0}\xi_N \tag{11}$$

$$\gamma_\alpha(t) = \exp\left(\frac{1}{16\pi^2}\int_{t_0}^{t} G_\alpha(t)\,dt\right) = \prod_{j=1}^{3}\left(\frac{\alpha_{j,0}}{\alpha_j}\right)^{c_\alpha^j/2b_j} \tag{12}$$

$$\xi_i = \exp\left(\frac{1}{16\pi^2}\int_{t_0}^{t}\lambda_i^2 dt\right). \tag{13}$$

It is obvious that the ratio of bottom and tau Yukawa couplings at any scale depends on the integral [29]:

$$\xi_N = \exp\left(\frac{1}{16\pi^2}\int_{t_0}^{t}\lambda_N^2 dt\right). \tag{14}$$

In the absence of neutrino couplings, this factor is equal to one. However, when $\lambda_{N_0} \neq 0$, ξ_N becomes lower than one and affects the unification conditions. The quantity (14) therefore plays a key role in our subsequent analysis.

At this stage, we need to remember that the b–τ equality at the GUT scale refers to the $(3,3)$ entries of the charged-lepton and down-quark mass matrices, whereas the detailed structure of the mass matrices may not be predicted by the GUT without some extra assumption(s), as discussed in the previous and subsequent sections. Therefore, it is relevant to assume mass textures with the property that the $(m_E^{diag})_{33}$ and $(m_D^{diag})_{33}$ entries are no longer equal after diagonalization at the GUT scale [29]. To understand the effect, we consider a 2×2 example, and assume that the off-diagonal terms in the down-quark mass matrix m_D are small compared to the (33) element, whereas this is not the case for the charged-lepton mass matrix. In this case, one can approximate the down-quark and charged-lepton mass matrices at the GUT scale by

$$m_D^0 = A\begin{pmatrix} c & 0 \\ 0 & 1 \end{pmatrix}, \quad m_E^0 = A\begin{pmatrix} x^2 & x \\ x & 1 \end{pmatrix}, \tag{15}$$

where A may be identified with $m_b(M_{GUT})$, the bottom quark mass at the scale M_{GUT}. These textures ensure that $(m_D^0)_{33} = (m_E^0)_{33}$ at the GUT scale. Moreover, the form of m_E^0 is such that the hierarchical relation between the two mass eigenvalues is obtained, $m_3 \gg m_2$. Note that, in this simple example, we work with textures that are symmetric before renormalization, which affects differently the left- and right-handed states. At low energies, the eigenmasses are obtained by diagonalising the renormalized Yukawa matrices, which is equivalent to diagonalising the quark and charged-lepton Yukawa matrices at the GUT scale, and then evolving the eigenstates and the mixing angles separately. In this way, we see that the trace of the charged-lepton mass matrix, which gives the higher eigenvalue, is not 1 but $1 + x^2$, and therefore the effective λ_b and λ_τ are not equal after diagonalization.

To simplify our analysis, we assume that M_{ν_R} is diagonal with degenerate eigenvalues. For hierarchical neutrino masses, however, the results can be generalized for arbitrary heavy Majorana neutrino masses by using the results of Appendix B. Since we are working in the small-tan β regime, in which the renormalization-group effects of the charged-lepton Yukawa couplings can be neglected, it is easier to pass to a basis in which the Dirac neutrino-mass matrix is diagonal, by performing an SU(2)-invariant rotation of the Dirac mass matrices for charged and neutral leptons. In this basis, the renormalization-group effect of the potentially large neutrino Yukawa couplings in the run from M_{GUT} down to M_N is simply parametrized by the integral ξ_N.

Let us also assume that the initial neutrino texture at M_{GUT} is

$$m_\nu^D = B\begin{pmatrix} y^2 & y \\ y & 1 \end{pmatrix}, \tag{16}$$

leading to

$$m_{eff}^0 = m_\nu^D \cdot M_{\nu_R}^{-1} \cdot m_\nu^{D^T} = B^2(y^2+1)\begin{pmatrix} y^2 & y \\ y & 1 \end{pmatrix}. \tag{17}$$

It should be stressed that we have, in general, a relative phase between the (12) elements of the mass matrices m_ν^D and m_E^0. This phase should in principle be taken into account, since it determines whether the mixing between the charged-lepton and the neutrino sectors, is constructive or destructive [23]. Below, we take the mass matrix elements to be real numbers, so we need only consider the distinct cases $xy > 0$ and $xy < 0$. Since the matrix diagonalising m_{eff} is

$$V_\nu = \frac{1}{\sqrt{1+y^2}}\begin{pmatrix} 1 & -y \\ y & 1 \end{pmatrix}, \tag{18}$$

the form of m_E at the GUT scale is, in the basis where the neutrinos are diagonal,

$$m_E(M_{GUT}) = A\begin{pmatrix} a & \sqrt{ab} \\ \sqrt{ab} & b \end{pmatrix} \tag{19}$$

where

$$a \equiv (x-y)^2/(1+y^2), \quad b \equiv (xy+1)^2/(1+y^2). \tag{20}$$

Taking into account the running of the charged-lepton mass matrix, at the scale M_N one has:

$$m_E(M_N) = \tilde{A}\begin{pmatrix} a & \sqrt{ab} \\ \xi_N\sqrt{ab} & \xi_N b \end{pmatrix}, \tag{21}$$

where $\tilde{A}$ is a coefficient that contains flavour-independent renormalization-group effects, and ξ_N, (14) is the integral associated with the running of the neutrino Yukawa

coupling. Since $m_E(M_N)$ is non-symmetric, the left- and right-handed lepton mixing angles are different. The left-handed mixing angle at M_N is calculated by diagonalising the hermitian matrix $m_E(M_N)m_E^\dagger(M_N)$, and is given by

$$\sin 2\theta_{23}(M_N) = \frac{2\sqrt{ab}\xi_N}{a\ +\ \xi_N^2\ b}\ . \tag{22}$$

3.2 Neutrino renormalization below M_N

Before proceeding with the numerical analysis, for completeness we first discuss renormalization below the right-handed Majorana mass scale. Here, λ_N decouples and the relevant running is that of the effective neutrino mass operator:

$$8\pi^2\frac{d}{dt}m_{eff} = \left[-(\frac{3}{5}g_1^2 + 3g_2^2) + 3\lambda_t^2\right] m_{eff}\ . \tag{23}$$

This implies that an initial texture $m_{eff}(M_N)^{ij}$ at M_N becomes at a lower scale

$$m_{eff} \propto I_g \cdot I_t \cdot m_{eff}(M_N) \tag{24}$$

where we have not written explicitly the dependence on $I_i = exp[\frac{1}{8\pi^2}\int_{t_0}^{t}\lambda_i^2 dt]$, with the subindex i referring to the charged-lepton flavours e, μ and τ, and where

$$I_g = exp\left[\frac{1}{8\pi^2}\int_{t_0}^{t}(-c_i g_i^2 dt)\right] \tag{25}$$

$$I_t = exp\left[\frac{3}{8\pi^2}\int_{t_0}^{t}\lambda_t^2 dt\right]. \tag{26}$$

The running of the lepton mixing angle θ_{23} [30,31] is given by

$$16\pi^2\frac{d}{dt}\sin^2 2\theta_{23} = 2\sin^2 2\theta_{23}(1-2\sin^2\theta_{23}) \times(\lambda_\tau^2 - \lambda_\mu^2)\frac{m_{eff}^{33}+m_{eff}^{22}}{m_{eff}^{33}-m_{eff}^{22}}.$$

We see from (27) that, for small $\tan\beta$, the renormalization effects on the mixing are small below M_N, reflecting the stability of the texture. Thus, in practice, the mixing freezes at the scale M_N and the angle defined in (22) is the one we compare with the low-energy data on mixing in the lepton sector. However, the exact values of the neutrino masses depend on I_g and I_t.

3.3 Conditions for maximal mixing

The best fit to the Super-Kamiokande data is obtained for a value of the mixing angle in the lepton sector $\sin 2\theta_{23}$ close to unity: $\sin^2 2\theta_{23} > 0.9$. We see from (22) that the requirement of maximal mixing, $\sin 2\theta_{23} = 1$, is equivalent to the condition

$$\sqrt{a} = \sqrt{b}\ \xi_N. \tag{27}$$

Using the expressions (20) for a and b, we rewrite this expression as

$$x - y = \pm\ \xi_N\ (xy + 1). \tag{28}$$

There are two solutions for this equation, associated with the two signs of the square roots, which should be chosen in such a way that $|x|$ and $|y|$ are less than one. Hence the requirement of maximal mixing, $\sin 2\theta_{23} \simeq 1$, is equivalent to the relations

$$y = \frac{x-\xi_N}{1+\xi_N\ x} \qquad \text{for} \quad x \geq 0$$
$$y = \frac{x+\xi_N}{1-\xi_N\ x} \qquad \text{for} \quad x \leq 0. \tag{29}$$

Therefore, the requirement of maximal mixing at low energies gives a simple relation between the entries of the neutrino and charged-lepton mass matrices at high energies, as a function of the neutrino renormalization-group factor ξ_N, which, as we shall show, is bounded by $1 > \xi_N > 0.8$.

4 Numerical analysis

We use two different codes for our numerical analysis, one taking a bottom-up and the other a top-down approach to gauge- and Yukawa-coupling unification [5]. We use the two-loop renormalization-group evolution of the gauge and Yukawa couplings in both programs, except for the running of m_{eff}, where we use one-loop formulae. In the range between M_{GUT} and M_N, we take into account the running of λ_N, and run with the supersymmetric β functions. At the scale M_N, the effective lepton mixing freezes, as mentioned earlier, but the evolution of m_{eff} still has to be taken into account, since it changes the magnitudes of the neutrino mass eigenvalues. Thus, between M_N and M_{SUSY} we include the running of m_{eff} and continue to run with the supersymmetric β functions. Below M_{SUSY}, we run with the Standard Model β functions, and continue to include the running of m_{eff}, which is now described by the equation

$$16\pi^2\frac{dm_{eff}}{dt} = (-3g_2^2 + 2\lambda + 2S)m_{eff} \tag{30}$$

where λ is the Higgs coupling: $M_H^2 = \lambda v^2$, and $S \equiv 3\lambda_t^2$ [30]. Finally, for the running between M_Z and m_b, we take into account the decoupling of both λ_t and g_2 from the running of the couplings.

As a basis for our numerical studies, we first consider evolution of the (33) matrix elements as if these were equal to the heavier eigenvalues of the mass matrices, i.e., ignoring mixing effects in the runs. Furthermore, we do not demand precise unification of couplings, but we choose a scale $M_{GUT} \simeq 1.5\ 10^{16}$ GeV, for which approximate

[5] As already remarked, we have checked that the inclusion of neutrinos in the renormalization-group equations for the gauge couplings does not greatly affect the conditions for gauge unification.

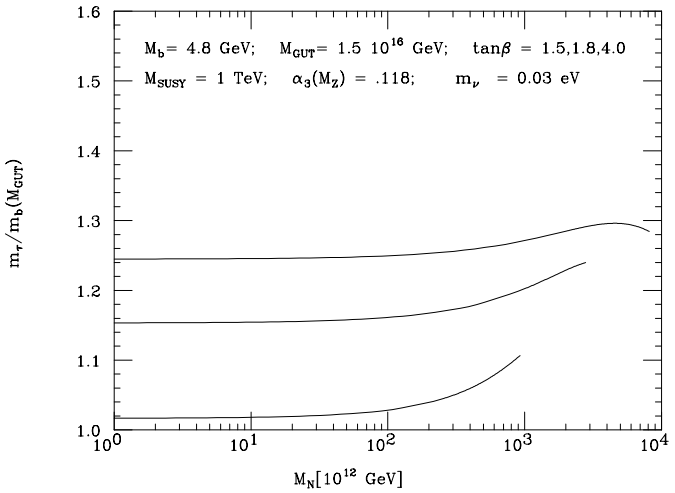

Fig. 1. The ratio $m_\tau/m_b(M_{GUT})$ as a function of M_N, with the choice $m_\nu = 0.03$ eV and for different values of $\tan\beta$: from bottom to top, $\tan\beta = 1.5$, 1.8 and 4, respectively

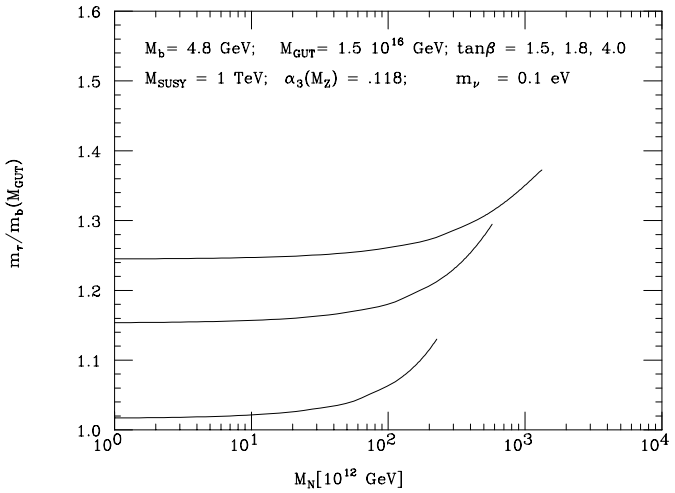

Fig. 2. The ratio $m_\tau/m_b(M_{GUT})$ as a function of M_N, with the choice $m_\nu = 0.1$ eV, for the same values of $\tan\beta$, from bottom to top, as in Fig. 1

unification of the three gauge couplings holds at the few per-mille level for all the cases analysed in this article. We choose a characteristic soft supersymmetry breaking scale of the order of 1 TeV, at which we decouple all supersymmetric particles, and for which approximate unification of gauge couplings can be achieved for values of $\alpha_3(M_Z) \simeq 0.118$ [4]. The top-quark mass has been fixed to 175 GeV and the pole bottom-quark mass to 4.8 GeV, where we use the two-loop QCD relations between running and pole masses. We then plot the ratio $m_\tau/m_b(M_{GUT})$, as a function of M_N, for fixed values of the light neutrino mass m_ν and of $\tan\beta$. This is shown in Figs. 1, 2 and 3 for the neutrino mass values $m_\nu = 0.03$, 0.1 and 1 eV, respectively. In each figure, the lines are truncated when the value of M_N is such that the neutrino Yukawa coupling enters the non-perturbative regime at scales below $M_{GUT} : \lambda_N^2(M_N)/4\pi \simeq 1$ [6]

Later we will reinterpret the results of the figures taking into account the mixing effects in the running, but already at this stage we can make some interesting observations:

(i) For small λ_N, corresponding in the see-saw model to small M_N, the appearance of the neutrino masses does not play a major role. Therefore, for small values of $\tan\beta$ in the region of the top-quark mass infrared fixed-point solution, we obtain $b-\tau$ unification, from which we see a deviation as $\tan\beta$ increases.

(ii) As λ_N becomes larger for fixed $\tan\beta$, corresponding to a larger M_N in the see-saw model, the neutrino coupling lowers λ_τ with respect to λ_b. Therefore, in order to obtain the correct value of m_b/m_τ at low energies, we need to start with lower values of $\lambda_b/\lambda_\tau(M_{GUT})$.

[6] In this analysis, we have ignored the threshold corrections to the fermion Yukawa couplings induced by the squark and slepton mixing parameters, since these corrections are strongly model dependent and small at these values of $\tan\beta$, and therefore they do not affect the overall picture displayed in Figs. 1, 2 and 3 [41,42].

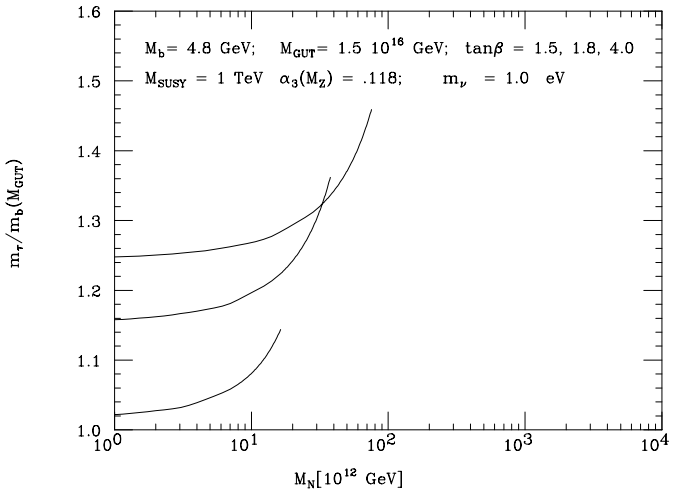

Fig. 3. The ratio $m_\tau/m_b(M_{GUT})$ as a function of M_N, with the choice $m_\nu = 1$ eV, for the same values of $\tan\beta$, from bottom to top, as in Fig. 1

(iii) As the coupling λ_N increases, we expect that at some stage the corresponding value of M_N gets so close to the GUT scale that, after reaching a peak, the effects on $b-\tau$ unification decrease again, because of their dependence on $\ln(M_N/M_{GUT})$. This explains the behaviour of $m_\tau/m_b(M_{GUT})$ for the choice $\tan\beta = 4$ in Fig. 1. For the other values of $\tan\beta$ displayed in Fig. 1, and also for all values of $\tan\beta$ displayed in Figs. 2 and 3, the Dirac neutrino coupling is so large that λ_N enters the non-perturbative regime before this peak is reached.

(iv) As stated above, in Fig. 3 we present, for completeness, the results on $m_\tau/m_b(M_{GUT})$ for a neutrino mass $m_\nu = 1$ eV. Such a value of the neutrino mass is not compatible with the assumption of hierarchical neutrino masses which we favour in this paper. However, Fig. 3 serves to document the important constraints on parameter space that are imposed in this case by requiring that

one avoids the non-perturbative regime. We do not analyze this value of m_ν any further in this paper.

4.1 Neutrino mixing effects

The main effects of the neutrino Yukawa couplings on the running of the lepton Yukawa coupling matrix elements have been presented in (21). In the above, when plotting the ratio of the bottom to tau Yukawa couplings, we worked in the basis in which the neutrinos are diagonal, and ignored the mixing in the charged-lepton sector. We now discuss how to interpret the precise unification relation of the (33) elements in the down-quark and charged-lepton sectors in view of the results shown in Figs. 1 and 2.

In the presence of lepton mixing, and in the basis in which the neutrino Dirac mass matrix is diagonal, the quantity that is renormalized in the way displayed in the figures as the tau Yukawa coupling is in fact the (33) element of the charged-lepton mass matrix. Hence, if we denote by $\tilde{m}_\tau$ the extrapolated value of the τ mass shown in the figures, the value of the (33) element at the GUT scale is given in the presence of mixing by

$$(m_E)_{33}(M_{GUT}) = \tilde{m}_\tau(M_{GUT}) \times \frac{(m_E)_{33}}{m_\tau} \qquad (31)$$

or, equivalently,

$$(m_E)_{33}(M_{GUT}) = \tilde{m}_\tau(M_{GUT}) \times \frac{\xi_N\, b}{\sqrt{(a+b)(a+b\xi_N^2)}}\,. \qquad (32)$$

Since $(m_E)_{33}(M_{GUT}) = A\, b$ in this basis, we find

$$\frac{\tilde{m}_\tau(M_{GUT})}{A} = \frac{\sqrt{(a+b)(a+\xi_N^2 b)}}{\xi_N}. \qquad (33)$$

Hence, in the presence of mixing in the lepton sector, we *expect* a mismatch of the extrapolated value of the τ Yukawa coupling, as given by the above expression.

The factor ξ_N can be obtained simply from the figures, by observing that the difference between the extrapolated values of $\tilde{m}_\tau$ for vanishing and non-vanishing neutrino Yukawa couplings is given, at one-loop, by $1/\xi_N$. Hence, for the same value of $\tan\beta$, one should take the obtained value of $\tilde{m}_\tau/m_b$ for a given value of M_N and divide it by its value at low values of $M_N \lesssim 10^{12}$ GeV to obtain, in a very good approximation, the desired factor $1/\xi_N$.

4.2 $b-\tau$ unification and maximal mixing

We now combine the above information with the condition of maximal mixing. Substituting the value of y required for maximal mixing, (29), one obtains,

$$a = \frac{\xi_N^2\,(x^2+1)}{\xi_N^2+1}$$
$$b = \frac{1+x^2}{\xi_N^2+1}. \qquad (34)$$

Further substituting these expressions into (33), one obtains

$$\frac{\tilde{m}_\tau(M_{GUT})}{m_b(M_{GUT})} = (1+x^2)\sqrt{\frac{2}{1+\xi_N^2}}, \qquad (35)$$

where we have assumed that unification takes place as described in (15): $m_b(M_{GUT}) = A$. Since $0.8 > \xi_N > 1$, the ratio $\tilde{m}_\tau/m_b$ at M_{GUT} given by (35) must be close to $(1+x^2)$.

We may now address the question of unification. We use the results of Fig. 1 to specify the value of x for which one obtains the desired unification relation. For this, one has first to read the value of ξ_N from the figure, as explained before, and then compare the obtained value of $\tilde{m}_\tau/m_b$ with (35). Since all the values of $\tilde{m}_\tau(M_{GUT})/m_b(M_{GUT})$ encountered in Fig. 1 are lower than 1.5, a solution for x consistent with unification can always be obtained. With this solution at hand, one can determine from (29) the value of y needed to obtain maximal mixing.

For instance, for low values of $\tan\beta$ close to the fixed point, and low values of $M_N \simeq 10^{12}$ GeV, we find that $\xi_N \simeq 1$ and $b-\tau$ mass unification demands $x \simeq 0$. Thus, all the mixing should be located in the neutrino sector in the original basis at the scale M_{GUT}. On the contrary, for the same value of $\tan\beta$, but larger values of M_N $(1/\xi_N)$ for which unification of neutrino and top Yukawa coupling can take place, we find that $x \simeq 0.25$–0.3 and therefore $y \simeq -(0.5$–$0.55)$, so moderate mixing in both the lepton Dirac mass matrices is required at the GUT scale.

We summarize in Tables 5 and 6 the values of x and y needed to obtain mass unification for a neutrino mass of order 0.03 eV. The same is done in Tables 7 and 8 for a neutrino mass of order 0.1 eV. We observe that the range of values of x and y needed to achieve unification depends strongly on $\tan\beta$, but does not depend much on the exact value of the neutrino mass. For a given value of $\tan\beta$, the values of x and y depend, in a first approximation, only on the product $m_\nu \times M_N$ [7].

4.3 On the unification of λ_N and λ_t

In $SO(10)$ models, in which the third generation Yukawa couplings appear from the $SO(10)$ invariant Yukawa interaction $\mathbf{16}_3\mathbf{10}\mathbf{16}_3$, not only the bottom and Yukawa couplings unify, but also the neutrino and the top Yukawa couplings take equal value at M_{GUT} [27,28]. It is therefore interesting to see when unification of the neutrino and the top-quark Yukawa couplings takes place. Since we are working in the basis in which the neutrino and top-quark Dirac mass matrices are diagonal, unification takes place when the ratio of the neutrino to the top-quark Yukawa

[7] Although we do not discuss this case in detail, we comment that, at large $\tan\beta$, bottom-τ unification is consistent with neutrino masses, even in the absence of lepton mixing, as a result of the bottom Yukawa coupling effects and the corrections from sparticle loops to m_b (for a discussion of these effects see, for example, [5]).

Table 5. Values of x leading to $b-\tau$ Yukawa coupling unification for $m_\nu = 0.03$ eV, for different choices of $\tan\beta$ and M_N

$M_N[10^{13}$ GeV]	1	10	20	50	70	150	250	400
$\tan\beta = 1.5$	0.13	0.15	0.17	0.21	0.23			
$\tan\beta = 1.8$	0.39	0.40	0.40	0.41	0.42	0.43	0.44	
$\tan\beta = 4.0$	0.50	0.50	0.50	0.50	0.50	0.51	0.52	0.52

Table 6. Values of y leading to $b-\tau$ Yukawa coupling unification for $m_\nu = 0.03$ eV, for different choices of $\tan\beta$ and M_N

$M_N[10^{13}$ GeV]	1	10	20	50	70	150	250	400
$\tan\beta = 1.5$	-0.77	-0.73	-0.69	-0.62	-0.58			
$\tan\beta = 1.8$	-0.44	-0.43	-0.42	-0.40	-0.39	-0.37	-0.35	
$\tan\beta = 4.0$	-0.34	-0.33	-0.33	-0.32	-0.32	-0.31	-0.30	-0.29

Table 7. Values of x leading to $b-\tau$ Yukawa coupling unification for $m_\nu = 0.1$ eV, for different choices of $\tan\beta$ and M_N

$M_N[10^{12}$ GeV]	1	10	50	80	100	200	400	800
$\tan\beta = 1.49$	0.13	0.14	0.17	0.18	0.20	0.26		
$\tan\beta = 1.8$	0.39	0.39	0.40	0.41	0.41	0.43	0.45	
$\tan\beta = 4.0$	0.50	0.50	0.50	0.50	0.50	0.51	0.52	0.54

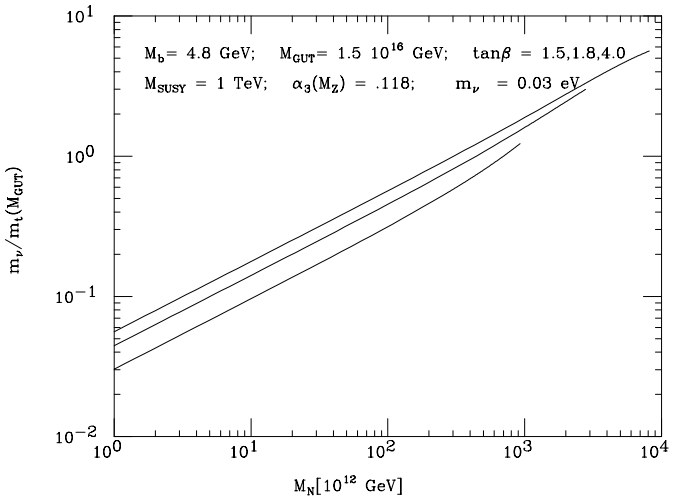

Fig. 4. The ratio $m_\nu/m_t(M_{GUT})$ as a function of M_N, with the choice $m_\nu = 0.03$ eV, for the same values of $\tan\beta$, from bottom to top, as in Fig. 1

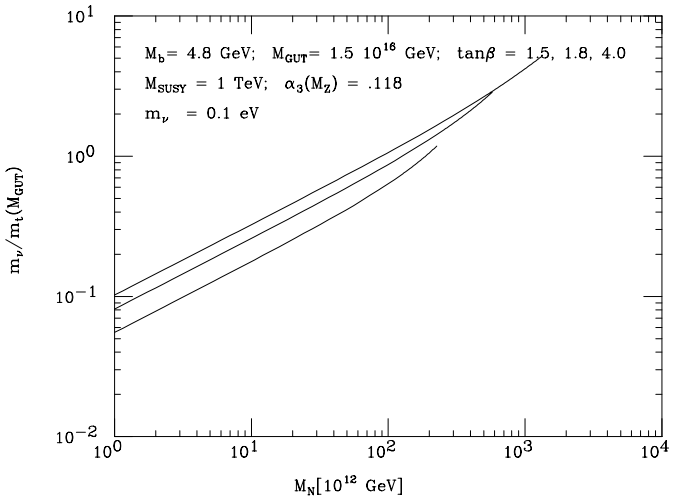

Fig. 5. The ratio $m_\nu/m_t(M_{GUT})$ as a function of M_N, with the choice $m_\nu = 0.1$ eV, for the same values of $\tan\beta$, from bottom to top, as in Fig. 1

couplings is given by

$$\frac{\lambda_N(M_{GUT})}{\lambda_t(M_{GUT})} = 1 + y^2. \tag{36}$$

One can now use the values of y displayed in the Tables 6 and 8 to investigate the values of M_N for which $b-\tau$ and $t-\nu$ unification take place as a function of $\tan\beta$ and M_N.

Figures 4 and 5 show the behaviour of the ratio of the neutrino Yukawa coupling to the top Yukawa coupling at the scale M_{GUT}. Close to the infrared fixed point of the top-quark mass: $\tan\beta \simeq 1.5$, $t-\nu$ Yukawa unification can only take place at large values of M_N for which the neutrino Yukawa coupling becomes strong, namely, for values $M_N \simeq 9\ 10^{14}$ GeV and $M_N \simeq 2.2\ 10^{14}$ GeV for $m_\nu = 0.03$ eV and $m_\nu = 0.1$ eV, respectively. For $m_\nu = 0.03$ eV and $\tan\beta = 1.8$ ($\tan\beta = 4$) $t-\nu$ Yukawa unification can be achieved for $M_N \simeq 5\ 10^{14}$ GeV ($M_N \simeq 3.5\ 10^{14}$ GeV). For $m_\nu = 0.1$ eV, instead, and $\tan\beta = 1.8$ ($\tan\beta = 4$), $t-\nu$

Table 8. Values of y leading to $b-\tau$ Yukawa coupling unification for $m_\nu = 0.1$ eV, for different choices of $\tan\beta$ and M_N

$M_N[10^{12}$ GeV]	1	10	50	80	100	200	400	800
$\tan\beta = 1.49$	-0.76	-0.75	-0.70	-0.66	-0.62	-0.52		
$\tan\beta = 1.8$	-0.44	-0.43	-0.42	-0.41	-0.40	-0.37	-0.33	
$\tan\beta = 4.0$	-0.34	-0.34	-0.33	-0.33	-0.32	-0.31	-0.29	-0.26

Yukawa unification can be achieved for $M_N \simeq 1.4\ 10^{14}$ GeV ($M_N \simeq 1.0\ 10^{14}$ GeV).

5 Comparison with textures derived from exact $SU(5)$ relations

In the above, we have analyzed the consequences of assuming quark and lepton mass matrix textures that are generated via higher-order operators, and hence violate the exact $SU(5)$ relation between the left-handed lepton and right-handed down-quark sectors. This relation could be fulfilled by taking, for instance, the following mass matrix textures at the GUT scale [21,22]

$$m_D^0 = A \begin{pmatrix} 0 & 0 \\ x & 1 \end{pmatrix}, \quad m_E^0 = A \begin{pmatrix} 0 & x \\ 0 & 1 \end{pmatrix}. \tag{37}$$

We assume that the neutrino mass matrix at the GUT scale is still symmetric and parametrized by the parameter y, as in (16). In the basis in which the neutrinos are diagonal, the lepton mass matrix takes the form

$$m_E(M_{GUT}) = \frac{A}{1+y^2} \begin{pmatrix} -y(x-y) & x-y \\ -y(xy+1) & xy+1 \end{pmatrix} \tag{38}$$

and hence, following the same procedure as in the previous case, we find that the low-energy form of the lepton mass matrix is given by

$$m_E(M_N) = \frac{\tilde{A}}{1+y^2} \begin{pmatrix} -y(x-y) & x-y \\ -\xi_N y(xy+1) & \xi_N(xy+1) \end{pmatrix}. \tag{39}$$

From the above, we obtain the following value of the lepton mixing angle $\sin 2\theta_{23}$:

$$\sin 2\theta_{23} = 2\xi_N \frac{(x-y)(xy+1)}{\xi_N^2(xy+1)^2 + (x-y)^2} \tag{40}$$

which is exactly the same as in (22). Hence the conditions for maximal mixing are satisfied for exactly the same relation between y and x as in (29). However, the relation between the extrapolated value of $\tilde{m}_\tau(M_{GUT})$ and the coefficient A is different. Indeed, using the same notation as before, one obtains

$$\frac{\tilde{m}_\tau(M_{GUT})}{A} = \frac{\sqrt{a+\xi_N^2 b}}{\xi_N}\ . \tag{41}$$

Analogously to the charged-lepton sector, the down-quark sector at low energies is now given by

$$m_D(\mu) \simeq \begin{pmatrix} 0 & 0 \\ I_t^{1/3}\xi_t x & I_t^{1/3}\xi_t \end{pmatrix} \tag{42}$$

and therefore the left-handed mixing angle is equal to zero, while the extrapolated value of the bottom Yukawa coupling at M_{GUT}, $\tilde{m}_b(M_{GUT})$, is related to the (33) element of the down quark mass matrix by

$$(m_D)_{33}(M_{GUT}) = \tilde{m}_b(M_{GUT})\frac{(m_D)_{33}}{m_b} \equiv A \tag{43}$$

or, equivalently,

$$(m_D)_{33}(M_{GUT}) = \frac{\tilde{m}_b}{\sqrt{x^2+1}} \equiv A. \tag{44}$$

Equating the values of A in (44) and (41), we obtain

$$\frac{\tilde{m}_\tau(M_{GUT})}{\tilde{m}_b(M_{GUT})} = \frac{1}{\xi_N}\sqrt{\frac{a+\xi_N^2 b}{1+x^2}}\ . \tag{45}$$

Finally, for the values of x and y which fulfill the condition (29) of maximal mixing, we obtain

$$\frac{\tilde{m}_\tau(M_{GUT})}{\tilde{m}_b(M_{GUT})} = \sqrt{\frac{2}{1+\xi_N^2}}. \tag{46}$$

The main difference between (35) and (46) resides in the fact that the factor $(1+x^2)$ does not appear in the latter. This is just a reflection of the structure of the down and lepton quark masses at the GUT scale. Moreover, (46) is independent of x, although it implicitly assumes that the condition (29) for maximal mixing is fulfilled. Since the factor $\sqrt{2/(1+\xi_N^2)} \leq 1/\xi_N$, it follows from Fig. 1 that approximate unification can be achieved only for values of $\tan\beta$ consistent with the infrared fixed-point solution for the top-quark mass. Moreover, for the condition of unification of the top-quark and neutrino Yukawa couplings at the top quark mass fixed point solution, for which $\xi_N \simeq 0.87$, unification can only be achieved for somewhat larger values of the bottom mass (or lower values of $\alpha_3(M_Z)$) than the one used in Fig. 1, namely $M_b \simeq 5.1$ GeV corresponding to values of $m_b(M_b) \simeq 4.5$–4.6 GeV. These values of the bottom mass, although high, are still consistent with phenomenological constraints. In this sense, the situation is better than the case where there is no mixing in the lepton sector, for which unacceptable values of $m_b(M_b) \simeq 4.8$–4.9 GeV would be required in order to achieve $b-\tau$ and $t-\nu_\tau$ unification [27,28].

6 Conclusions

In this paper, we analyzed quark-lepton mass unification in the light of the evidence of neutrino oscillations coming from the recent Super-Kamiokande data. We mainly concentrated on $b-\tau$ Yukawa coupling unification, but have also examined $t-\nu$ Yukawa unification in the small and moderate $\tan\beta$ regime of the MSSM. We have shown that, in the case that there is only small right-and left-handed mixing in the down-quark sector, Yukawa coupling unification can be achieved for values of $\tan\beta$ larger than those consistent with the infrared fixed-point solution of the top-quark mass. Although, for simplicity, we analysed the case of symmetric mass matrices at the scale M_{GUT}, this result can be easily generalized to the general case of non-symmetric lepton mass matrices, leading to a large hierarchy between the Dirac mass eigenvalues. On the other hand, if exact $SU(5)$ relations between the right-handed down-quark and left-handed charged-lepton mass matrices are used, Yukawa coupling unification can be achieved only for small values of $\tan\beta \simeq 1.5$, close to the infrared fixed-point solution for the top-quark mass.

These results cast in a new light the theoretical interest of intermediate values of $\tan\beta$, which had previously been disfavoured on the basis of Yukawa coupling unification arguments. We now see that there is a subtle interplay between these arguments and neutrino masses and mixing, which opens up new possibilities at intermediate $\tan\beta$.

One significant implication of these results is for Higgs searches at LEP. In the absence of lepton mixing, for small values of $\tan\beta$ consistent with $b-\tau$ mass unification, values of the Higgs mass in the unexcluded range 95–105 GeV still accessible to LEP could be obtained only for large values of the stop masses and of the stop mixing parameter [42]. On the other hand, at large $\tan\beta$, the Higgs mass tends naturally to values which are beyond this range, unless one of the stops is relatively light and the stop mixing parameter is small (as happens, for instance, in scenarios consistent with electroweak baryogenesis [43]). The range $95 \leq m_h \leq 105$ GeV of Higgs masses is achieved most naturally for intermediate values $2 \leq \tan\beta \leq 4$. Therefore, finding the a Higgs boson in this mass range at LEP would probably hint towards either a light stop, or such intermediate values of $\tan\beta$. As we have shown in this article, $b-\tau$ Yukawa coupling unification can still be achieved for $2 \leq \tan\beta \leq 4$ if the mass-matrix textures at M_{GUT} are such that the left- and right-handed down-quark mixing is small, whereas the expected large mixing in the lepton sector is shared between the neutrino and the charged-lepton sector, with a significant contribution from the latter. Thus, there is an intriguing theoretical linkage between neutrino physics and the Higgs search at LEP, which passes via mass unification.

Acknowledgements. We thank G.F. Giudice for useful discussions. C.W. would also like to thank S. Raby for very stimulating discussions. Work supported in part by the US Department of Energy, Division of High Energy Physics, under Contract W-31-109-ENG-38.

Appendix A. Lowering $\tan\beta$ in $SO(10)$ models

In this appendix we present a mechanism to lower the predicted value of $\tan\beta$ in the framework of SO(10) models, like the ones considered in this article. Low values of $\tan\beta$ can easily be achieved by assuming that only one **10** of GUT Higgs fields couples to fermions, but that this **10** contains only some components of the two electroweak Higgs doublets, the other components coming, for instance, from an additional **10** [36]. The overall effect is to multiply the down and lepton mass matrices by a factor ω, which is the ratio of the relative components of the two Higgs doublets in the **10** which couples to fermions. The minimal model would hence be obtained for $\omega = 1$. Here, in order to obtain $\omega > 1$, we may implement a slightly modified version of the mechanism implemented in [36], as we now describe.

Consider the superpotential

$$W = \mathbf{10}\,\mathbf{45}_{B-L}\mathbf{10}^{'} + \left[M_1\,\mathbf{10} + (M_2 + \mathbf{45}_X)\,\mathbf{10}^{'}\right]\mathbf{10}^{''}, \tag{47}$$

where M_1 and M_2 are of order M_{GUT}, $\mathbf{10}$, $\mathbf{10}^{'}$ and $\mathbf{10}^{''}$ are decuplets, and only $\mathbf{10}$ participates in the fermion mass operators.

The first term in W implements the $SO(10)$ missing-doublet mechanism [40], and yields 4 light doublets: 2, $\bar{\mathbf{2}}$, $\mathbf{2}^{'}$ and $\bar{\mathbf{2}}^{'}$, whereas the corresponding color triplets acquire a mass of order M_{GUT}. The second term gives a mass to a linear combination of 2 and $\mathbf{2}^{'}$, by pairing it with $\bar{\mathbf{2}}^{''}$, and a different linear combination of $\bar{\mathbf{2}}$ and $\bar{\mathbf{2}}^{'}$, by pairing it with $\mathbf{2}^{''}$. Explicitly, the light states are given by

$$\mathbf{2}_L = \frac{M_1\,\mathbf{2}^{'} - (M_2 + \mathbf{v})\,\mathbf{2}}{\sqrt{M_1^2 + (M_2 + \mathbf{v})^2}} \tag{48}$$

and

$$\bar{\mathbf{2}}_L = \frac{M_1\,\bar{\mathbf{2}}^{'} - (M_2 - \mathbf{v})\,\bar{\mathbf{2}}}{\sqrt{M_1^2 + (M_2 - \mathbf{v})^2}}, \tag{49}$$

where $< \mathbf{45}_X >= \mathbf{v} \times X$, with $X = +\,(-)$ when it acts on the $SU(5)$ $\mathbf{5}$ ($\bar{\mathbf{5}}$) components of a $\mathbf{10}$ representation, respectively. Since $\mathbf{2}$ couples to the up quarks and $\bar{\mathbf{2}}$ couples to the down quarks, in this example we have

$$\lambda_t = \lambda \frac{M_2 + \mathbf{v}}{\sqrt{M_1^2 + (M_2 + \mathbf{v})^2}},$$
$$\lambda_b = \lambda \frac{M_2 - \mathbf{v}}{\sqrt{M_1^2 + (M_2 - \mathbf{v})^2}}, \tag{50}$$

and

$$\omega = \frac{M_2 - \mathbf{v}}{M_2 + \mathbf{v}} \times \frac{\sqrt{M_1^2 + (M_2 + \mathbf{v})^2}}{\sqrt{M_1^2 + (M_2 - \mathbf{v})^2}}. \tag{51}$$

Notice that, in this simple example, M_1 cannot be too small, or else a pair of light triplets would appear in the

spectrum, affecting the prediction for $\sin^2\theta_W$. This restriction does not apply to $M_2 - \mathbf{v}$, as long as $M_2 + \mathbf{v}$ is still of the order of the GUT scale.

Appendix B. On the mixing in the heavy majorana sector

In this appendix we generalize the analysis presented in this article, for the general case of hierarchical Dirac mass matrices for charged leptons and neutrinos, and non-vanishing mixing in the heavy Majorana neutrino sector. Considering a symmetric mass matrix for the Majorana neutrinos at the GUT scale, of the form

$$\mathcal{M}_N(M_{GUT}) = M \begin{pmatrix} f & g \\ g & h \end{pmatrix}, \tag{52}$$

we transform it to the basis in which the Dirac neutrino-mass matrix is diagonal. In this basis, the Majorana mass of the neutrinos will take a form

$$\mathcal{M}'_N(M_{GUT}) = M \begin{pmatrix} f' & g' \\ g' & h' \end{pmatrix} \tag{53}$$

where we do not write out the formal expressions of the matrix elements as functions of f, g and h, since they are not essential for our discussion. In the same basis, the Dirac mass matrix of the neutrinos is given approximately by $m_\nu^D = \mathrm{diag}(0, B(1+y^2))$. The evolution of the mass matrix, (53) to the relevant Majorana mass scale leads to

$$\mathcal{M}'_N(M_N) = M \begin{pmatrix} f' & g'\xi_N^2 \\ g'\xi_N^2 & h'\xi_N^4 \end{pmatrix} \tag{54}$$

where the scale M_N should be identified with the inverse of $(\mathcal{M}_N^{-1})_{33}$. If we now compute the effective low-energy Majorana mass for the left-handed neutrinos, we obtain

$$m'_{eff}(M_N) = \lambda_N^2 H_2^2 \cdot (\mathcal{M}_N^{-1})_{33} \begin{pmatrix} 0 & 0 \\ 0 & 1 \end{pmatrix} \tag{55}$$

with

$$(\mathcal{M}_N^{-1})_{33} = \frac{f'}{(f'h' - g'^2)\xi_N^4}. \tag{56}$$

The important thing to notice is that, as in the case of a unit Majorana neutrino-mass matrix, no mixing in the neutrino sector is induced. So, in the case of hierarchical Dirac neutrinos, the mixing in the heavy Majorana sector does not affect the observed lepton mixing at low energies [23].

We observe that the above conclusion was obtained by approximating the smallest neutrino mass to zero. In the more realistic case of a small but non-vanishing neutrino mass, the above conclusion holds unless $g' \gg f', h'$, since then the approximations made in the above analysis would be invalid. Therefore, the analysis presented in this article holds in the quite general case considered in this article, in which the hierarchy of neutrino masses is induced by the Dirac mass structure and the elements of the heavy Majorana mass matrix are of the same order (with $\det\mathcal{M}_N \neq 0$), independently of the mixing in the Majorana mass sector.

References

1. M.S. Chanowitz, J. Ellis, M.K. Gaillard, Nucl. Phys. B **128** (1977) 506; A.J. Buras, J. Ellis, M.K. Gaillard, D.V. Nanopoulos, Nucl. Phys. B **135** (1978) 66; D.V. Nanopoulos, D.A. Ross, Nucl. Phys. B **157** (1979) 273
2. J. Ellis, D.V. Nanopoulos, S. Rudaz, Nucl. Phys. B **202** (1982) 43; D.V. Nanopoulos, D.A. Ross, Phys. Lett. 108B (1982) 351 and 118B (1982) 99
3. H. Arason, D. Castano, B.Keszthelyi, S. Mikaelian, E. Piard, P. Ramond, B. Wright, Phys. Rev. Lett. 67 (1991) 2933; V. Barger, M.S. Berger, P. Ohmann, Phys. Rev. D47 (1993) 1093; P. Langacker, N. Polonsky, Phys. Rev. D49 (1994) 1454
4. M. Carena, S. Pokorski, C.E.M. Wagner, Nucl. Phys. B406 (1993) 59
5. L.J. Hall, R. Rattazzi, U. Sarid, Phys. Rev. D50 (1994) 7048; M. Carena, M. Olechowski, S. Pokorski, C.E.M. Wagner, Nucl. Phys. B **419** (1994) 213 and Nucl. Phys. B **426** (1994) 269
6. H. Georgi, D.V. Nanopoulos, Nucl. Phys. B **159** (1979) 16; H. Georgi, C. Jarlskog, Phys. Lett. 86B (1979) 297
7. J. Ellis, M.K. Gaillard, Phys. Lett. 88B (1979) 315
8. Y. Fukuda et al., Super-Kamiokande Collaboration, Phys. Lett. B433 (1998) 9; Phys. Lett. B436 (1998) 33; Phys. Rev. Lett. 81 (1998) 1562
9. S. Hatakeyama et al., Kamiokande Collaboration, Phys. Rev. Lett. 81 (1998) 2016; M. Ambrosio et al., MACRO Collaboration, Phys. Lett. B434 (1998) 451
10. The literature on the subject is vast. Some of the basic references are: C. D. Froggatt, H. B. Nielsen, Nucl. Phys. B147 (1979) 277; H. Fritzsch, Phys. Lett. 70B (1977) 436; B73 (1978) 317; Nucl. Phys. B155 (1979) 189; J. Harvey, P. Ramond, D. Reiss, Phys. Lett. B92 (1980) 309; S. Dimopoulos, L. J. Hall, S. Raby, Phys. Rev. Lett. 68 (1992) 1984; C. Wetterich, Nucl. Phys. B261 (1985) 461; L. Ibanez, G.G. Ross, Phys. Lett. B332 (1994) 100
11. G.K. Leontaris, D.V. Nanopoulos, Phys. Lett. B212 (1988) 327; Y.Achiman, T. Greiner, Phys. Lett. B329 (1994) 33; Y. Grossman, Y. Nir, Nucl. Phys. B448 (1995) 30; H. Dreiner et al., Nucl. Phys. B436 (1995) 461; P. Binétruy, S. Lavignac, P. Ramond, Nucl. Phys. B477 (1996) 353; G.K. Leontaris, et al., Phys. Rev. D53 (1996) 6381; P. Binétruy et al, Nucl. Phys. B496 (1997) 3; S. Lola, J.D. Vergados, Progr. Part. Nucl. Phys. 40 (1998) 71; J.K. Elwood, N. Irges, P. Ramond, Phys. Lett. B413 (1997) 322 and Phys. Rev. Lett. 81 (1998) 5064; S. Lavignac, N. Irges, P. Ramond, Phys. Rev. D58 (1998) 035003
12. Z. Maki, M. Nakagawa, S. Sakata, Prog. Theor. Phys. 28 (1962) 247
13. M. Apollonio et al., Chooz Collaboration, Phys. Lett. B420 (1998) 397

14. See for example, L. Wolfenstein, Phys. Rev. D17 (1978) 20; S. P. Mikheyev, A. Yu Smirnov, Yad. Fiz. 42 (1985) 1441; Sov. J. Nucl. Phys. 42, 913 (1986)
15. C. Athanassopoulos et al., LSND Collaboration; Phys. Rev. C54 (1996) 2685; Phys. Rev. Lett. 77 (1996) 3082; Phys. Rev. Lett. 81 (1998) 1774
16. K. Eitel et al., Nucl. Phys. Proc. Suppl. 70 (1999) 210
17. M. Gell-Mann, P. Ramond, R. Slansky, proceedings of the Stony Brook Supergravity Workshop, New York, 1979, eds. P. Van Nieuwenhuizen and D. Freedman (North-Holland, Amsterdam)
18. J. Ellis, S. Lola, hep-ph/9904279
19. A. Casas, J.R. Espinosa, A. Ibarra, I. Navarro, hep-ph/9905381, hep-ph/9905381 and hep-ph/9906281
20. See for example: C.H. Albright, S.M. Barr, Phys. Rev. D58 (1998) 013002; C.H. Albright, K.S. Babu, S.M. Barr, Phys. Rev. Lett. 81 (1998) 1167; J. K. Elwood, N. Irges, P. Ramond, Phys. Rev. Lett. 81 (1998) 5064; Y. Nomura, T. Yanagida, Phys. Rev. D59 (1999) 017303; Q. Shafi, Z. Tavartkiladze, hep-ph/9811282; Z. Berezhiani, A. Rossi, hep-ph/9811447; T. Blazek, S. Raby, K. Tobe, hep-ph/9903340
21. K. Hagiwara, N. Okamura, Nucl. Phys. B548 (1999) 60
22. G. Altarelli, F. Feruglio, Phys. Lett. B451 (1999) 388
23. S. Lola, G.G. Ross, hep-ph/9902283, to appear in Nucl. Phys. B
24. P. Langacker, N. Polonsky, Phys. Rev. D47 (1993) 4028
25. P. Langacker, N. Polonsky, Phys. Rev. D52 (1995) 3082
26. W. A. Bardeen, M. Carena, S. Pokorski, C. E. M. Wagner, Phys. Lett. B320 (1994) 110
27. F. Vissani, A. Yu. Smirnov, Phys. Lett. B **341** (1994) 173
28. A. Brignole, H. Murayama, R. Rattazzi, Phys. Lett. B **335** (1994) 345
29. G.K. Leontaris, S. Lola, G.G. Ross, Nucl. Phys. B454 (1995) 25
30. K. Babu, C. N. Leung, J. Pantaleone, Phys. Lett. B **319** (1993) 191
31. P.H. Chankowski, Z. Pluciennik, Phys. Lett. B **316** (1993) 312; M. Tanimoto, Phys. Lett. B360 (1995) 41
32. J. Ellis, G.K. Leontaris, S. Lola, D.V. Nanopoulos, hep-ph/9808251, to appear in Eur. J. Phys. C
33. N. Haba, N. Okamura, M. Sugiura, hep-ph/9810471
34. J.A. Harvey, P. Ramond, D. Reiss, Nucl. Phys. B199 (1982) 223
35. G. Anderson, S. Raby, S. Dimopoulos, L. Hall, G. Starkman, Phys. Rev. D **49** (1994) 3660
36. M. Carena, S. Dimopoulos, C.E.M. Wagner, S. Raby, Phys.Rev. D52 (1995) 4133
37. B.C. Allanach, S.F. King, G.K. Leontaris, S. Lola, Phys. Rev. D56 (1997) 2632 and Phys. Lett. B407 (1997) 275
38. See for example the work by G. Altarelli, F. Feruglio, Phys. Lett. B439 (1998) 112; JHEP 9811 (1998) 021 and references therein
39. K.S. Babu, J.C. Pati, F. Wilczek, hep-ph/9812538
40. S. Dimopoulos, F. Wilczek, The Unity Of The Fundamental Interactions, Proceedings of the 1981 Erice Summer School, Ed. A. Zichichi, 237
41. J.A. Casas, J.R. Espinosa, H.E. Haber, Nucl. Phys. B526 (1998) 3
42. M. Carena, P. Chankowski, S. Pokorski, C.E.M. Wagner, Phys. Lett. B441 (1998) 205
43. M. Carena, M. Quiros, C.E.M. Wagner, Nucl. Phys. B524 (1998) 3